

Interaction of phosphorus with dislocations in heavily phosphorus doped silicon

著者	Ohno Y., Shirakawa T., Taishi T., Yonenaga I.
journal or publication title	Applied Physics Letters
volume	95
number	9
page range	091915
year	2009
URL	http://hdl.handle.net/10097/51710

doi: 10.1063/1.3224184

Interaction of phosphorus with dislocations in heavily phosphorus doped silicon

Y. Ohno,^{a)} T. Shirakawa, T. Taishi, and I. Yonenaga

Institute for Materials Research, Tohoku University, Katahira 2-1-1, Aoba-ku, Sendai 980-8577, Japan

(Received 7 July 2009; accepted 18 August 2009; published online 4 September 2009)

Effects of annealing at 1173 K, that is comparable to the typical temperatures for the fabrication of Si-based devices, on the dissociated dislocations in Czochralski-grown silicon crystals heavily doped with phosphorus atoms were determined. Dislocation segments with edge component are constricted. They climbed out of the slip plane toward the compression side, forming complete dislocation segments. The dissociation width of the rest segments is increased. These results suggest that phosphorus atoms segregate nearby dislocations and the high doping level at the dislocations lowers the formation energy of negatively charged vacancies. © 2009 American Institute of Physics. [DOI: 10.1063/1.3224184]

Dislocations are still being of considerable importance in silicon (Si) technology. Even though dislocation-free bulk Si crystals, grown by the Czochralski (CZ) method, are commercially available, dislocations are frequently introduced during device fabrication processes; that is, ion implantation used to make shallow junctions or heavily doped regions, and annealing at elevated temperatures (typically above 1073 K) for dopant diffusion, oxidation, or nitridation. Also, dislocations are inevitably introduced, at the present moment, in strained Si epilayers for high carrier mobility devices,^{1,2} cast Si for solar cells,^{3,4} and so forth. They play a crucial role on the mechanical and electronic properties of Si-based devices since they act as segregating centers to point defects such as dopant atoms and vacancies, as well as fast paths for diffusing atoms,⁵ and also they introduce defect levels in the band gap. Understanding the interactions of dislocations with point defects is, therefore, necessary to improve the performance of Si-based devices.

The interactions have been studied for more than three decades,⁶ and recently, they have been evaluated quantitatively; for instance, the interaction of a dislocation with a defect that acts as locking agent for dislocation motion is estimated experimentally,⁷ and it is theoretically expected that point defects are energetically more stable nearby dislocation cores^{8–12} and stacking faults¹³ with respect to a crystalline environment. However, the interactions, especially in heavily doped CZ-Si crystals, have not been fully explored. This paper reports transmission electron microscopy (TEM) works concerning the structural characteristics of dislocations in CZ-Si crystals heavily doped with phosphorus (P) atoms, that are commonly used as a *n*-type dopant in Si, after the annealing at an elevated temperature, which is comparable to the typical temperatures used in the fabrication processes of Si-based devices. It is proposed that the segregation of P atoms on a dislocation results in the reduction of the formation energy of a vacancy nearby the dislocation.

Bulk single crystals of Si doped with P atoms with the concentration of $3 \times 10^{18} \text{ cm}^{-3}$ and those of undoped Si were grown by the conventional CZ method. The CZ specimens necessarily contained oxygen (O) atoms with the concentration of about 10^{18} cm^{-3} , even though O atoms were

not doped intentionally. No dislocation was detected in the specimens by x-ray topography and the etch pit method. They were deformed by applying a compressive stress along $[12\bar{3}]$, and dislocations lying on (111) were introduced. The compression tests were conducted at elevated temperature 1173 K for about 30 min (up to a shear strain of about 10%), in a flowing high-purity argon gas atmosphere, resulting in a dislocation density of about $10^8\text{--}10^9 \text{ cm}^{-2}$. The specimens were then cooled slowly without stress by removing the heat source. Before the cooling, some specimens were annealed at 1173 K up to 10 h without stress, in the same atmosphere as the compression tests. They were thinned for TEM by mechanochemical etching, without ion milling, so that the irradiation induced effects on dislocations could be ignored. The structural nature of the sample was characterized by TEM with a 120 keV electron beam.

Most dislocations in as-deformed specimens were dissociated into partial dislocations bounding stacking faults, as reported,^{14,15} with the Burgers vector \mathbf{b} of $a/6\langle 112 \rangle$. In P-doped specimens, dislocations were constricted over long segments of the dislocation line, forming complete dislocation segments with $\mathbf{b}=a/2\langle 110 \rangle$, by annealing at 1173 K.

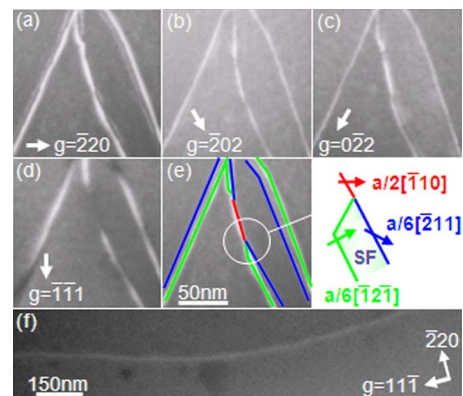


FIG. 1. (Color online) TEM images of a P-doped Si annealed for 3 h after deformation; taken with the reflection \mathbf{g} of (a) $[220]$, (b) $[202]$, (c) $[022]$, and (d) $[111]$ ($4\mathbf{g}$ diffraction condition, the deviation parameter is $1.4 \times 10^{-2} \text{ \AA}^{-1}$). (e) A schematic view of the structural nature of the dislocations in (a). (f) A TEM image of an undoped Si annealed for 10 h after deformation ($\mathbf{g}=[111]$).

^{a)}Electronic mail: yutakaohno@imr.tohoku.ac.jp.

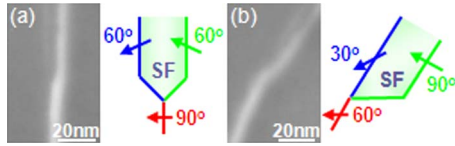


FIG. 2. (Color online) A TEM image of the node between a dissociated segment and a constricted one; with (a) 90° (edge) or (b) 60° orientation. The inset in each figure shows a schematic view of the geometry of the node.

The dissociated segments and constricted ones were clearly distinguished by a weak-beam TEM technique,¹⁶ as shown in Fig. 1; pairs of partial segments [Figs. 1(b) and 1(c)] and stacking faults [Fig. 1(d)], as well as complete segments, were separately observable. No extended defect of another type, such as SiO_2 (Ref. 17) and SiP precipitate,¹⁸ was observed. The total length of constricted segments increased with increasing annealing time, and about 40% of dislocations were constricted at 10 h. On the other hand, dislocations in undoped specimens were not constricted by the annealing [e.g., see the long stacking fault ribbon bounded by a dissociated dislocation in Fig. 1(f)].

The geometry of the node between a dissociated segment and a constricted one varied depending on the line orientation α , defined as the angle of \mathbf{b} to \mathbf{u} for the constricted segment, in which \mathbf{u} is the unit vector along the positive direction of the dislocation line. For $\alpha \sim 90^\circ$, i.e., for dislocations with edge orientation, the geometry was symmetric; a pair of 60° partial segments were combined and converted into a complete segment at the middle of the pair [Fig. 2(a)]. When $0^\circ \ll \alpha \ll 90^\circ$, the geometry was asymmetric. The typical example was dislocations with $\sim 60^\circ$ orientation [$\alpha \sim 60^\circ$, Figs. 2(b) and 1(a)]. A pair of 30° and 90° partial segments were combined at the location close on the 30° partial. No node for $\alpha \sim 0^\circ$ was observed; dislocations with screw orientation were not constricted. These results indicate that constricted segments have edge component and the constriction takes place via the movement of 60° and 90° partial segments, rather than that of 30° ones.

Constricted segments of a dislocation climbed out of the slip plane toward the compression side, i.e., vacancies were accumulated into the compression side, as shown in Fig. 3. Three-dimensional TEM revealed that constricted segments in the figure, that were invisible in Fig. 3(b), climbed toward

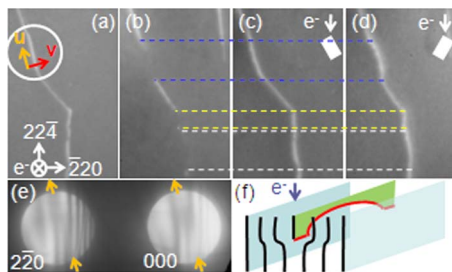


FIG. 3. (Color online) TEM images of a dislocation taken with $\mathbf{g} =$ (a) $[2\bar{2}0]$, (b) $[22\bar{4}]$, (c) $[\bar{1}31]$, and (d) $[\bar{3}1\bar{1}]$ (2g diffraction condition). (c) and (d) are a pair of stereo micrographs taken with an electron beam inclined by $\pm 31^\circ$ from $[111]$ toward $[2\bar{2}0]$. The vector \mathbf{v} is defined as $\mathbf{v} = \mathbf{u} \times \mathbf{c}$, in which \mathbf{c} is the unit vector pointing from the center of the illuminated specimen area to the focus position of the incident beam. (e) A CBED pattern obtained from the encircled area in (a). (f) A schematic view of atomic planes around a constricted segment in (a). The red curve indicates the dislocation line.

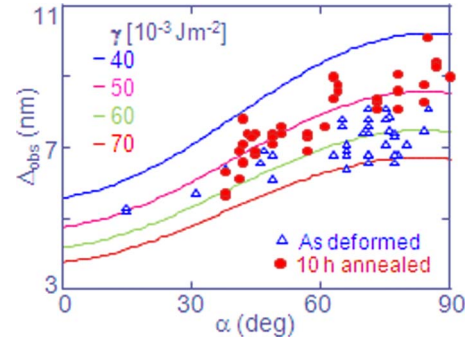


FIG. 4. (Color online) The separation of dissociated dislocations Δ_{obs} vs line orientation α . Open triangles and closed circles mean the data for as-deformed specimens and specimens annealed for 10 h after deformation, respectively. The curves give theoretical values for different stacking fault energy γ .

the electron incident surface [Figs. 3(c) and 3(d)]. The sense of the bend of a reflection line in the positive side of \mathbf{v} was the opposite of the sense of \mathbf{g} in a convergent-beam electron diffraction (CBED) pattern obtained from a constricted segment [Fig. 3(e)], and an extra half plane at the segment, therefore, expanded toward the electron incident surface,¹⁹ as shown schematically in Fig. 3(f). Climbing of dissociated dislocations without constriction, induced by the segregation of O atoms,¹⁷ was not observed in the present work.

The separation of dissociated segments Δ_{obs} , defined as the separation of the intensity peaks on weak-beam micrographs, was estimated for as-deformed specimens. The separation Δ_{obs} in P-doped specimens (triangles in Fig. 4) was about 8 nm for dislocations close to edge orientation ($\alpha \sim 90^\circ$). The Δ_{obs} decreased with decreasing α , and it was about 5 nm for dislocations close to screw orientation ($\alpha \sim 0^\circ$). The stacking fault energy γ was estimated as 50–70 mJ m^{-2} by using an anisotropic elasticity theory taking into account the deviation parameter.¹⁶ Similar result was obtained for undoped specimens (not shown). In P-doped specimens, Δ_{obs} for any line orientation increased with increasing annealing time; Δ_{obs} increased by about 20% at 10 h (circles in Fig. 4), and γ was reduced to 40–60 mJ m^{-2} . On the other hand, Δ_{obs} did not change by the annealing in undoped specimens (not shown).

The effects of P dopant on the separation of dissociated segments are discussed. The effects have been determined for dislocations introduced freshly in “pure” Si, that is, Si crystals grown by the floating-zone (FZ) method.^{14,15} In P-doped FZ-Si deformed at elevated temperature of 1073 K, that is close to the deformation temperature in the present work, the separation increases with increasing P concentration,¹⁴ and it increases by about 20% at 10^{19} cm^{-3} (10^{20} cm^{-3}).²⁰ It is considered that the phenomenon is due to P atoms segregated nearby dislocations during deformation, as indicated experimentally^{7,14} and theoretically,¹² and the separation is actually independent of P concentration when the deformation temperature is too low to migrate P atoms (633 K).¹⁵ Similarly, the separation in P-doped CZ-Si would increase by annealing at 1173 K due to the segregation of P atoms via the migration of P atoms since P atoms can move by 60 nm after annealing for 10 h (Ref. 21) and the P concentration nearby dislocations can increase to more than 10^{20} cm^{-3} . The separation did not change in undoped CZ-Si annealed at the same condition, and it is irrespective of the

oxygen effects such as the formation of SiO₂ precipitates and the segregation nearby dislocations. One possible mechanism for the increase of separation is the Coulomb repulsion in dissociated dislocations. Dislocations can be negatively charged via the displacement of the Fermi level due to P donors (Patel effect²²) since they act as acceptors.²³ Also, it is expected that P atoms segregate on stacking faults, bounded by partial dislocations, and they become negatively charged.¹⁰ Another possible mechanism is the reduction of stacking fault energy²⁴ induced by P atoms on stacking faults. In either event, segregation of P atoms nearby dislocations would be essential, even though their atomistic structure remains obscure.

Finally, we discuss the origin of the dislocation climb in CZ-Si induced by annealing at 1173 K. Similar climb takes place in undoped FZ-Si, even though the annealing temperature needed for the climb is rather high (1623 K); dissociated segments with edge component climb by the annealing, forming constricted segments, and the node between a dissociated segment and a constricted one is symmetric for dislocations with edge orientation.²⁵ The phenomenon is presumably due to the agglomeration of intrinsic vacancies via their thermal migration and the formation of vacancies nearby the dislocations, since the dominant point defect is the vacancy at temperatures above 1073 K.²⁶ Actually, the formation energy for a vacancy in the perfect crystal E_{bulk} is higher than that on dislocations ($\sim 1/3E_{\text{bulk}}$ for 90° partials,⁸ $\sim 2/3E_{\text{bulk}}$ for 30° partials⁹) and on stacking faults ($\sim 9/10E_{\text{bulk}}$),¹³ and vacancies should agglomerate nearby dissociated dislocations. Also, the agglomeration rate of vacancies nearby 90° partials would differ from that nearby 30° partials, due to the difference of the formation energy of a vacancy, and this would result in the formation of asymmetric nodes for dislocations with $\sim 60^\circ$ orientation. In the present work, the effect of the agglomeration of intrinsic vacancies via their thermal migration would be negligible since the annealing temperature of 1173 K was much lower than 1623 K. Dislocations did not climb in undoped CZ-Si at 1173 K, as well as in undoped FZ-Si at similar temperature.²⁵ Therefore, it is considered that the formation energy of a vacancy nearby a dislocation is reduced when P atoms are combined with the dislocation. This is consistent with the formation of negatively charged vacancies that were also concluded to mediate self-diffusion in Si under *n*-type doping conditions.²⁷ Further study, such as *in situ* observation of the dislocation climb, is necessary to elucidate in detail the climb mechanism.

In conclusion, structural characteristics of dislocations in heavily P-doped CZ-Si after annealing at 1173 K were determined. The separation of a dissociated segment increased with increasing annealing time, suggesting the segregation of P atoms nearby the dislocation via the thermal migration of P

atoms. Dissociated segments climbed out of the slip plane toward the compression side, suggesting that the formation energy of a vacancy nearby the segments is reduced via the formation of P-dislocation complexes. This finding may help to elucidate the multiple influence of dislocations and point defects on the physical properties of semiconductors.

This work was partially supported by the Ministry of Education, Culture, Sports, Science, and Technology, Japan, a Grant-in-Aid for Scientific Research (B), Grant No. 19310072 (2007–2009). The authors would like to thank Professor Shigeto R. Nishitani from Kwansai Gakuin University for useful discussions.

¹J. Parsons, R. J. H. Morris, D. R. Leadley, E. H. C. Parker, D. J. F. Fulgoni, and L. J. Nash, *Appl. Phys. Lett.* **93**, 072108 (2008).

²N. Usami, R. Nihei, I. Yonenaga, Y. Nose, and K. Nakajima, *Appl. Phys. Lett.* **90**, 181914 (2007).

³K. Hartman, M. Bertoni, J. Serdy, and T. Buonassisi, *Appl. Phys. Lett.* **93**, 122108 (2008).

⁴N. Usami, K. Kutsukake, K. Fujiwara, I. Yonenaga, and K. Nakajima, *Appl. Phys. Express* **1**, 075001 (2008).

⁵M. Legros, G. Dehm, E. Arzt, and T. J. Balk, *Science* **319**, 1646 (2008).

⁶As a review, H. Alexander, *Dislocations in Solids 7* (Elsevier, Amsterdam, 1986), p. 115.

⁷I. Yonenaga, *Mater. Sci. Eng., B* **124**, 293 (2005).

⁸M. M. de Araújo, J. F. Justo, and R. W. Nunes, *Appl. Phys. Lett.* **90**, 222106 (2007).

⁹J. F. Justo, M. de Koning, W. Cai, and V. V. Bulatov, *Phys. Rev. Lett.* **84**, 2172 (2000).

¹⁰J. F. Justo, A. Antonelli, T. M. Schmidt, and A. Fazzio, *Physica B* **273**, 473 (1999).

¹¹N. Lehto and S. Oberg, *Phys. Rev. B* **56**, R12706 (1997).

¹²M. Heggie, R. Jones, and A. Umerski, *Philos. Mag. A* **63**, 571 (1991).

¹³A. Antonelli, J. F. Justo, and A. Fazzio, *Phys. Rev. B* **60**, 4711 (1999).

¹⁴M. Sato, K. Sumino, and K. Hiraga, *Phys. Status Solidi A* **68**, 567 (1981).

¹⁵H. Gottschalk, *J. Phys.* **40**, C6 (1979).

¹⁶D. J. H. Cockayne, I. L. F. Lay, and M. J. Whelan, *Philos. Mag.* **20**, 1265 (1969).

¹⁷K. Minowa, I. Yonenaga, and K. Sumino, *Mater. Lett.* **11**, 164 (1991).

¹⁸Y. Zeng, X. Ma, W. Wang, D. Tain, L. Gong, and D. Yang, *J. Appl. Phys.* **105**, 093503 (2009).

¹⁹M. Tanaka, M. Terauchi, and M. Tsuda, *Convergent-Beam Electron Diffraction III* (JEOL, Tokyo, 1994), p. 178.

²⁰P atoms would segregate nearby dislocations during the introduction of the dislocations at 1073 K, and the P concentration nearby dislocations would be the order of 10^{20} cm^{-3} .

²¹R. N. Ghoshtagore, *Phys. Rev. B* **3**, 389 (1971).

²²J. R. Patel, L. R. Testardi, and P. E. Freeland, *Phys. Rev. B* **13**, 3548 (1976).

²³H. Ono and K. Sumino, *Jpn. J. Appl. Phys. Part 2* **19**, L629 (1980).

²⁴H. Suzuki, *J. Phys. Soc. Jpn.* **17**, 322 (1962).

²⁵I. L. F. Ray and D. J. H. Cockayne, *Proc. R. Soc. London, Ser. A* **325**, 543 (1971).

²⁶T. Abe, H. Harada, N. Ozawa, and K. Adomi, *Mater. Res. Soc. Symp. Proc.* **59**, 537 (1986).

²⁷H. Bracht, H. H. Silvestri, I. D. Sharp, and E. E. Haller, *Phys. Rev. B* **75**, 035211 (2007).